

## Seeded growth fabrication of Cu-on-Si electrodes for *in situ* ATR-SEIRAS applications

Hui-Feng Wang<sup>a</sup>, Yan-Gang Yan<sup>a</sup>, Sheng-Juan Huo<sup>a</sup>, Wen-Bin Cai<sup>a,b,\*</sup>,  
Qun-Jie Xu<sup>b</sup>, Masatoshi Osawa<sup>c</sup>

<sup>a</sup> Shanghai Key Laboratory for Molecular Catalysis and Innovative Materials and Department of Chemistry,  
Fudan University, Shanghai 200433, China

<sup>b</sup> Department of Environmental Engineering, Shanghai University of Electric Power, Shanghai 200090, China

<sup>c</sup> Catalysis Research Center, Hokkaido University, Sapporo 001-0021, Japan

Received 23 December 2006; received in revised form 14 March 2007; accepted 16 March 2007

Available online 20 March 2007

### Abstract

A seeded-growth approach has been developed to fabricate a Cu nanoparticle film (simplified hereafter with nanofilm) on Si for electrochemical ATR surface-enhanced infrared absorption spectroscopy (ATR-SEIRAS). The approach comprises an initial activation of the reflecting plane of hemicylindrical Si prism by introducing a Cu seed layer in a CuSO<sub>4</sub>-HF solution and the subsequent electroless deposition of the Cu nanofilms from an electroless Cu plating bath. The as-deposited Cu nanofilm exhibited strong SEIRA effect for the CO probe and interfacial free H<sub>2</sub>O. ATR-SEIRAS was also applied to characterize the adsorbed geometries of pyridine at the Cu/electrolyte interface. Only vibrational bands assignable to the A<sub>1</sub> symmetry modes were detected in the entire potential window investigated, suggestive of an end-on adsorption via the ring N-atom on a Cu electrode.

© 2007 Elsevier Ltd. All rights reserved.

**Keywords:** ATR-SEIRAS; Cu nanofilm electrode; Si; Seeded-growth; Carbon monoxide; Pyridine

### 1. Introduction

Because of its excellent electrical and thermal conductivity, mechanical workability, copper has found extensive applications varying from conventional pipelines for condensed water to advanced interconnects for ULSI chips [1–4]. The interfacial electrochemistry of a Cu electrode has gained great interest due to its practical importance in corrosion and inhibition [5–7], and electrocatalysis [8–10]. Electrochemical measurement [11,12] and surface-enhanced Raman spectroscopy (SERS) [13–19] have been employed chiefly for the study of adsorption and reaction at Cu electrodes. It is well known that electrochemical measurement provides the current-potential-time information about the electrochemical interface. SERS is very powerful in

probing the interface at the molecule-level, with merits of high sensitivity, capability of detecting low frequency vibrations, and far less interference from bulk water signal, as compared to conventional infrared absorption reflection spectroscopy (IRAS). Nevertheless, the complexity of the enhancement mechanisms of SERS, as well as the requirement of oxidation–reduction cycle (ORC) pretreatment in a chloride solution may compromise its versatility and strength [20].

Surface-enhanced infrared absorption spectroscopy (SEIRAS) with attenuated-total reflection (ATR) configuration is also an attractive analytical tool for probing electrochemical interfaces because of its high signal sensitivity and a simple surface selection rule [21–23]. A key issue for successfully implementing this technique is to fabricate appropriate nanoparticle metal films that can produce strong SEIRA effect while maintain essentially the same electrochemical properties as their bulk counterparts. Recently triggered by the effort in Osawa's group [24], simple wet fabrication techniques [25–40] (including chemical deposition and electrochemical deposition of metallic nanoparticle films on an IR window such as Si and

\* Corresponding author at: Shanghai Key Laboratory for Molecular Catalysis and Innovative Materials and Department of Chemistry, Fudan University, Shanghai 200433, China. Tel.: +86 21 55664050; fax: +86 21 65641740.

E-mail address: [wbcail@fudan.edu.cn](mailto:wbcail@fudan.edu.cn) (W.-B. Cai).

Ge) are developing rapidly, with an expectation to replace the traditional and expensive dry process fabrication (including vacuum evaporation and sputtering). A SEIRA-active Cu film chemically deposited on a Ge element has been reported [29]. However, Si is used more frequently than Ge as an IR element in electrochemical ATR-SEIRAS applications owing to its higher stability in acidic and neutral electrolytes over a much wider potential window. In fact, the electrochemistry of the desired metal over-films on Ge often suffers from abnormal responses, probably due to the dissolution of Ge substrate as well as the partial peeling of metal films. To our knowledge, wet process fabrication of Cu nanofilms on IR transparent Si for electrochemical ATR-SEIRAS has not been reported in the literature.

Most recently, a seeded-growth tactics was proposed in our group to fabricate the ATR-SEIRA-active Ag electrode on Si without the introduction of a second undesired metal (mostly Pd) as the catalytic seeds [40]. In this report we would like to extend this tactics to fabricate a Cu nanofilm electrode on Si for electrochemical ATR-SEIRAS application. Unlike chemical deposition of a Cu nanofilm on Ge in which the growth of a conductive and SEIRA-active Cu nanofilm occurs by the continuous dissolution of the Ge substrate via the displacement of Ge with Cu [41], our current approach allows a Cu nanofilm on Si to be deposited via initial activation with Cu seeds followed by its further growth in a Cu chemical plating bath without continuous dissolution of Si substrate. It should be emphasized that our seeded-growth tactics is quite different from that aimed for microelectronics application in which Pd [42] or Au [43] seeds were introduced to Si wafer surfaces as the catalysts, thus preventing possible contamination in the resultant Cu nanofilm electrode by a second metal.

The SEIRA activity of the chemically deposited Cu film on Si was examined by using CO as a probe molecule. Significantly enhanced IR absorption for surface species on the as-deposited Cu electrode enables to detect for the first time a band possibly due to interfacial free H<sub>2</sub>O co-existed with CO on the coinage metal. Meanwhile, as an initial move to extend the as-deposited Cu electrode to electrochemical ATR-SEIRAS application, the configuration of adsorbed pyridine (Py), a prototype molecule, was examined as well. The conclusion derived from present *in situ* SEIRAS is in accordance with that obtained from previous *in situ* SERS studies [14,15] as well as previous IRAS measurement in UHV [44] on Cu surfaces. However, the so-called  $\alpha$ -pyridyl species on Cu surfaces upon pyridine adsorption, deduced by *ex situ* SERS on Cu nanoparticles formed on an aluminum foil [18], was not discerned.

## 2. Experimental

### 2.1. Preparation and characterization of Cu nanofilm

The Cu nanofilm on Si was prepared as follows: the reflecting plane of a hemicylindrical Si prism was polished and then cleaned with the RCA method [45], then the total reflecting plane was immersed in 40% NH<sub>4</sub>F and 40% HF (10:1, v/v) solution for 2 min to terminate the Si surface with hydrogen. Cu seeds

were formed by immersing the Si reflecting plane in the 0.625 M HF solution containing 3.15 mM CuSO<sub>4</sub>·5H<sub>2</sub>O for 5–10 s. After thoroughly being rinsed with copious amount of ultrapure Milli-Q water, the electroless deposition of Cu nanofilms was carried out in a plating solution (recipe: 5 g L<sup>-1</sup> CuSO<sub>4</sub>·5H<sub>2</sub>O, 25 g L<sup>-1</sup> C<sub>4</sub>H<sub>4</sub>O<sub>6</sub>KNa·4H<sub>2</sub>O (i.e., potassium sodium tartrate), 10 mL L<sup>-1</sup> HCHO, 7 g L<sup>-1</sup> NaOH, adjusted to pH 12.5~13 with HCl) at 25–35 °C for 15–25 min. For comparison, Cu nanofilm on the reflecting plane of a Ge prism was prepared directly by immersing the latter in the above-mentioned plating solution at 25 °C for 20–25 min.

Inductively coupled plasma (ICP) atomic emission spectroscopy (AES) was used to estimate the thickness of the deposited Cu nanofilms by determining the concentrations of dissolved Cu ions from the Cu films on Si in hot aqua regia of a known volume. The average thickness of the Cu nanofilms was estimated to be around 68 nm, by assuming the same density as the bulk metals and using the geometric area for the calculations.

Atomic force microscopy (AFM) images of a Cu seed layer and Cu nanofilms on Si were acquired in tapping mode under ambient conditions with a Pico-SPM (Molecular Imaging, Tempe, AZ). Si cantilevers having spring constants of between 1.2 and 5.5 N m<sup>-1</sup> were used at resonance frequencies between 60 and 90 kHz.

The underpotential deposition (UPD) of Pb monolayer on the as-deposited Cu nanofilm electrode was carried out with cyclic voltammetry in a deaerated 0.1 M HClO<sub>4</sub> containing 1 mM Pb(ClO<sub>4</sub>)<sub>2</sub>·3H<sub>2</sub>O between -0.05 and -0.43 V (versus SCE) at 10 mV s<sup>-1</sup>. The average charge required for UPD of a Pb monolayer was used to estimate the surface roughness factor of the Cu nanofilm electrode.

### 2.2. *In situ* ATR-SEIRA spectroscopy

All the experiments were carried out at the room temperature. After being rinsed with ultrapure water, the above Cu-deposited Si prism was assembled to a spectroelectrochemical cell with which *in situ* ATR-SEIRAS measurement was carried out. A Pt gauze and a saturated calomel electrode (SCE) were used as the counter and reference electrodes, respectively. The Cu electrode was cleaned in 0.1 M KClO<sub>4</sub> by cycling it in between potentials of slight surface oxidation and hydrogen evolution followed with a cathodic reduction at -1.1 V for 2 min. The spectral measurements were performed with the Kretschmann ATR configuration, experimental details of which were described elsewhere [46]. Multi-step potential difference mode was used in which single-beam spectrum was taken at each potential of interest with respect to a suitable reference spectrum. For SEIRAS measurement of CO on Cu, CO gas (with a purity of 99.9%) was bubbled into the cell gently for 30 min to saturate 0.1 M KClO<sub>4</sub> with CO. The reference spectrum was taken at -0.6 V (SCE) in the same solution, at which the desorption of CO was virtually completed. The SEIRAS measurement of Py on Cu was carried out in a 0.1 M KClO<sub>4</sub> solution containing 10 mM pyridine with a reference spectrum taken in a 0.1 M KClO<sub>4</sub> solution without Py at each corresponding sample potential. All spectra are shown in the absorbance units defined as  $A = -\log(I/I_0)$ , where  $I$

and  $I_0$  represent the intensities of the infrared radiation reflected from the electrode at the sample potential and the reference one, respectively.

### 3. Results and discussion

#### 3.1. Electrochemical and AFM characterizations of a Cu nanofilm

Fig. 1 shows the typical cyclic voltammograms in between  $-1.0$  and  $0$  V for a polished Cu bulk electrode (dotted trace), a Cu nanofilm on Si electrode (dashed trace) and a Cu nanofilm on Ge electrode (solid trace), respectively, in  $0.1$  M  $\text{KClO}_4$  at  $50$   $\text{mV s}^{-1}$ . The surface roughness of the Cu massive electrode was not strictly controlled without being subjected to intensive polishing. Nevertheless, this did not prevent us from a qualitative comparison. It is revealed that the as-deposited Cu nanofilm on Si is much alike to the Cu bulk, while the Cu nanofilm on Ge suffers poor resemblance to the Cu bulk in terms of their electrochemical responses when the positive potential limit is relatively high. The reason may be ascribed to the dissolution of the less inactive Ge substrate (and thus possibly partial peeling of the Cu film) which distorts the overall electrochemical response of Cu film at least under the above conditions. Although there are some cases (not used in a wider potential range and/or in strong acid solutions) in which both Cu-on-Si and Cu-on-Ge electrodes may share rather comparable electrochemical responses, the above result suggests the necessity for developing ATR-SEIRA-active Cu electrodes on Si as a good addition.

Surface roughness factor of the as-deposited Cu nanofilm was estimated based on the averaged depositing and stripping charges for UPD of a Pb monolayer on Cu in  $0.1$  M  $\text{HClO}_4$  containing  $1$  mM  $\text{Pb}(\text{ClO}_4)_2 \cdot 3\text{H}_2\text{O}$  as shown in Fig. 2, by assuming a theoretical value of  $300$   $\mu\text{C cm}^{-2}$  for an ideal Cu(1 1 1) electrode as the reference [47,48]. The cyclic voltammetric feature of the above Pb-UPD on the as-deposited Cu film electrode is not identical to that on a polycrystalline Cu bulk electrode, rather it is somehow in between that on Cu(1 1 1) electrode and that

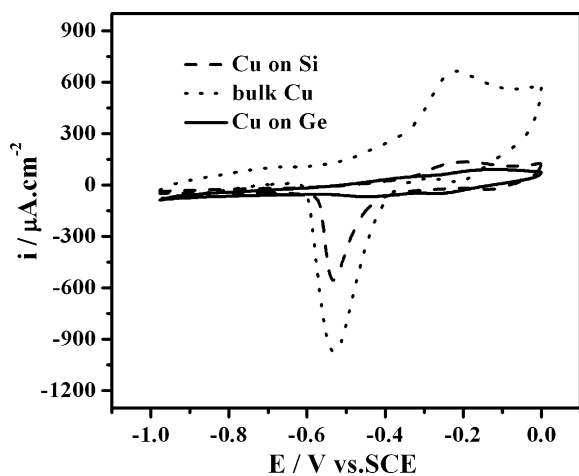


Fig. 1. Cyclic voltammograms for the chemically deposited Cu films on Ge (solid trace) and Si (dashed trace), and bulk Cu electrode (dotted trace) in deaerated neat  $0.1$  M  $\text{KClO}_4$ . Scan rate was  $50$   $\text{mV s}^{-1}$ .

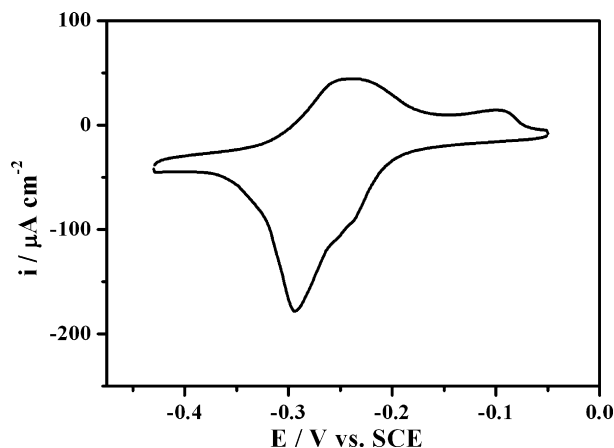


Fig. 2. Cyclic voltammogram for the UPD of a Pb monolayer on the Cu nanofilm electrode on Si in deaerated  $0.1$  M  $\text{HClO}_4$  containing  $1$  mM  $\text{Pb}(\text{ClO}_4)_2 \cdot 3\text{H}_2\text{O}$ , the scan rate is  $10$   $\text{mV s}^{-1}$ . The slightly larger deposition charge than stripping one is probably due to the partial Cu–Pb alloying at the initial deposition stage.

on Cu(1 1 0) electrode, suggestive of preferred growth to some extent of these two crystalline orientations [48]. As comparison, the corresponding cyclic voltammogram for Pb-UPD on a bulk polycrystalline Cu electrode is shown in Appendix A. The somewhat larger deposition charge than the stripping one is possibly due to the partial Cu–Pb alloying at the initial deposition stage, as also found in previous measurements on bulk Cu electrodes [47]. The average charge calculated from Fig. 2 is ca.  $780$   $\mu\text{C cm}^{-2}$ , yielding a roughness factor of ca. 2.6, which was slightly smaller than estimated for the Cu nanofilm on Ge [29].

The mechanism of the seeding process is believed as follows, which is associated with the dissolution of Si in the presence of  $\text{F}^-$  and a reduction of  $\text{Cu}^{2+}$ , i.e.,

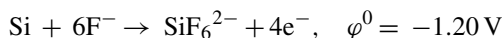
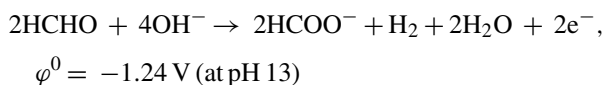


Fig. 3(a) shows the AFM image of the initial Cu seed layer on Si. It can be found that the Cu seed layer was composed of loosely packed ellipsoidal particles with an average lateral size of ca.  $80$  nm. These nanoparticles are not fully interconnected, and thus no significant electrical conductivity was detected for the entire film. Subsequent seeded growth of Cu particles occurs according to the following simplified reactions, i.e.,



The AFM image of the as-deposited Cu film on Si shown in Fig. 3(b) reveals an average lateral diameter of particles of ca.  $150$  nm and the feature height of ca.  $50$  nm. On the other hand, the mass equivalent thickness of the film estimated from ICP measurement was ca.  $68$  nm by taking the bulk Cu density for the calculation (i.e., by assuming Cu atoms being densely packed as in Cu crystals). Since the island film contains voids, it can reasonably be deduced that more than one layer of nanoparticles are

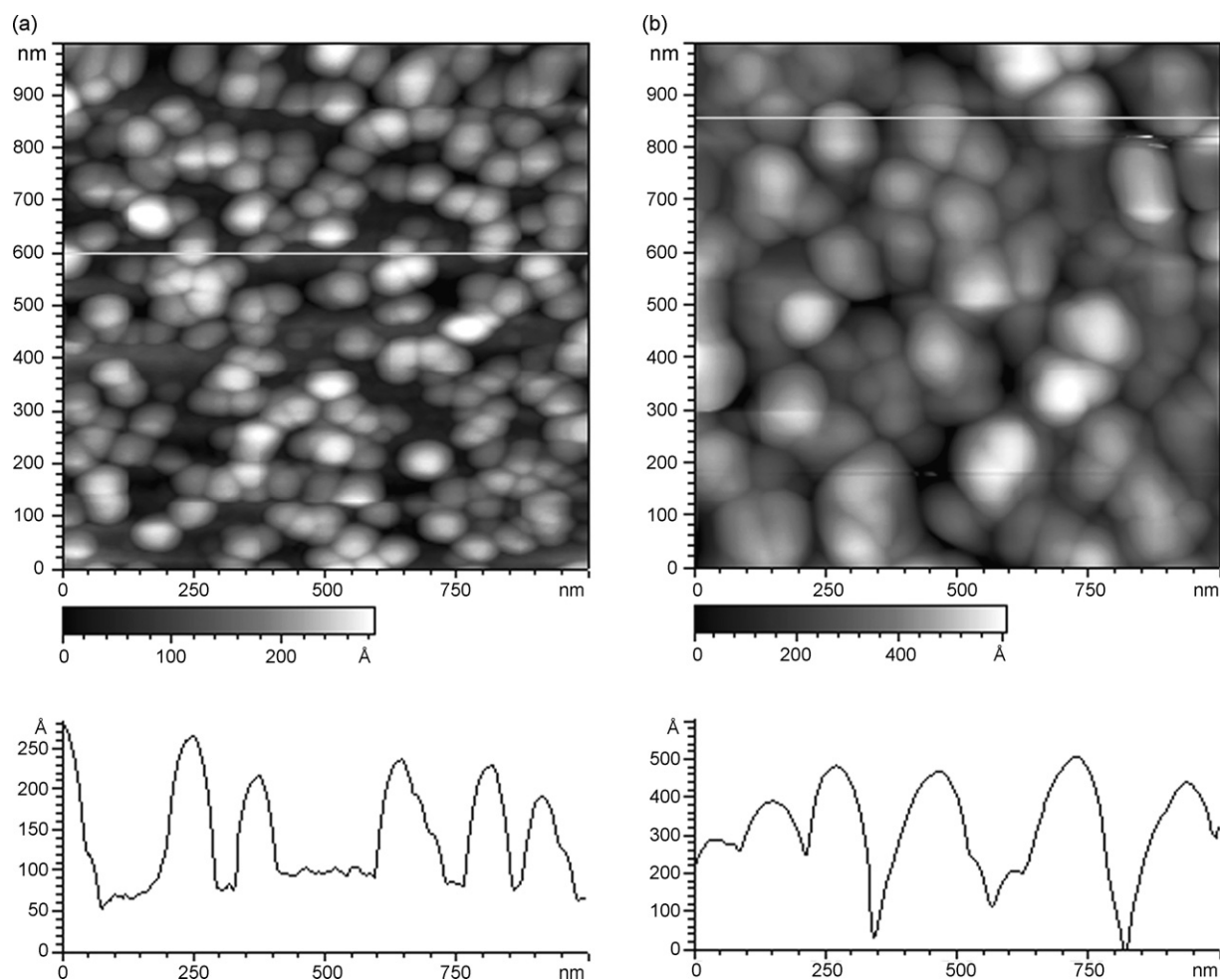


Fig. 3. AFM images for Cu seed layer (a) and Cu nanofilm (b) grown on Si.

packed and interconnected. In fact, the Cu nanofilms were shiny and quite homogeneous by eye-inspection and the conductivity was sufficient for (spectro)-electrochemical measurement.

### 3.2. *In situ* SEIRAS on Cu-on-Si electrode

Fig. 4 shows the cyclic voltammogram of the Cu electrode in Ar-saturated (solid trace) and CO-saturated (dotted trace) 0.1 M  $\text{KClO}_4$  solution with the initial potential at  $-0.5$  V, which is less positive than the potential of Cu oxidation. The hydrogen evolution current at potentials negative of  $-0.9$  V is markedly suppressed in the CO-saturated solution, suggestive of CO adsorption on the Cu electrode. The current suppression is not significant at potentials more positive than  $-0.9$  V, the reason of which can be understood by *in situ* ATR-SEIRAS measurement.

Shown in Fig. 5 are the potential-dependent SEIRA spectra for CO adsorption at the Cu electrode in CO-saturated 0.1 M  $\text{KClO}_4$  solution by taking the single-beam spectrum at  $-0.6$  V as the reference. Spectral collection was performed stepwise from the initial potential at  $-0.6$  V with a multi-step FTIR mode toward  $-1.3$  V. The band at  $2036\text{--}2080\text{ cm}^{-1}$  can be assigned to the linearly adsorbed CO on Cu. The asymmetric band shape with a tail at the low frequency side may be ascribed to the

inhomogeneity of the Cu nanoparticles. The  $\nu_{\text{CO}}$  band intensity increased as the potential moved negatively to  $-1.3$  V as shown in Fig. 6, in good agreement with that obtained by Kalaji and co-workers [49] and Miyake et al. [29]. This may be explained in

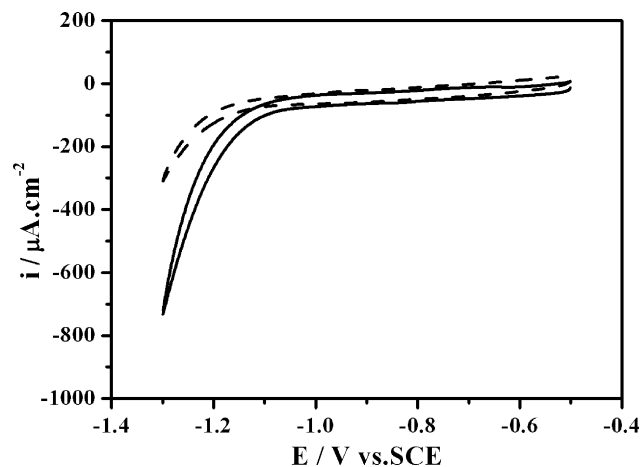


Fig. 4. Cyclic voltammograms for the chemically deposited Cu nanofilm in Ar-saturated (solid trace) and CO-saturated (dashed trace) 0.1 M  $\text{KClO}_4$ . Scan rate was  $50\text{ mV s}^{-1}$ .

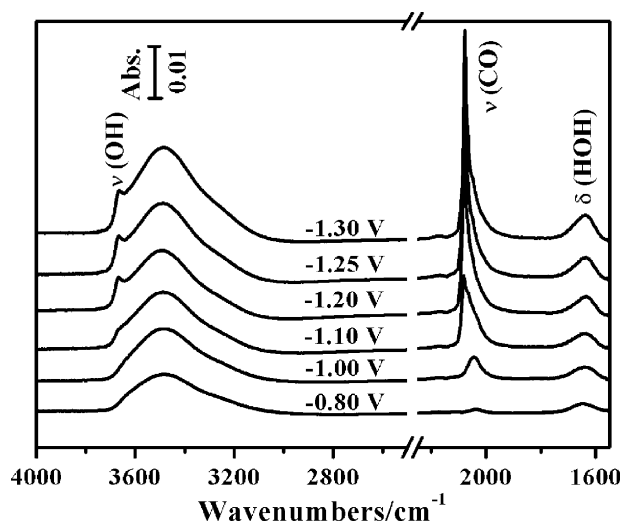


Fig. 5. Potential-dependent SEIRA spectra for CO adsorbed on the Cu electrode in 0.1 M KClO<sub>4</sub>. Sample spectra were taken at potentials indicated, and the reference spectrum at  $-0.6$  V.

considering that the desorption of anions (OH and/or ClO<sub>4</sub><sup>-</sup>) facilitates the adsorption of CO at potentials more negative than the pzc (ca.  $-0.8$  V) [50,51]. It is noted that the intensity of the  $\nu_{\text{CO}}$  band at  $-1.3$  V is 0.044 Abs, which far exceeded those reported for IRAS measurement on bulk Cu electrodes (0.001–0.002 Abs) [52], and was even somewhat larger than obtained for ATR-SEIRAS on a Cu-on-Ge electrode (0.025) [29]. After the appropriate calibration of the effects of surface roughness factor, surface coverage, incident angles and polarization states of IR radiation [33,40], the enhancement factor was estimated to be larger than 28.

Interestingly, a sharp band around  $3668\text{ cm}^{-1}$  was observed which was imposed on a broad band centered at ca.  $3500\text{ cm}^{-1}$ . The latter together with the  $\delta_{\text{HOH}}$  band at ca.  $1640\text{ cm}^{-1}$  could be assigned to the  $\nu_{\text{OH}}$  of interfacial H<sub>2</sub>O strongly hydrogen-bonded. Two possible surface OH-containing species may be ascribed to this band. The first is CuOH<sub>ads</sub> as suggested by Kalaji and co-workers [49]. However, they reported that this species

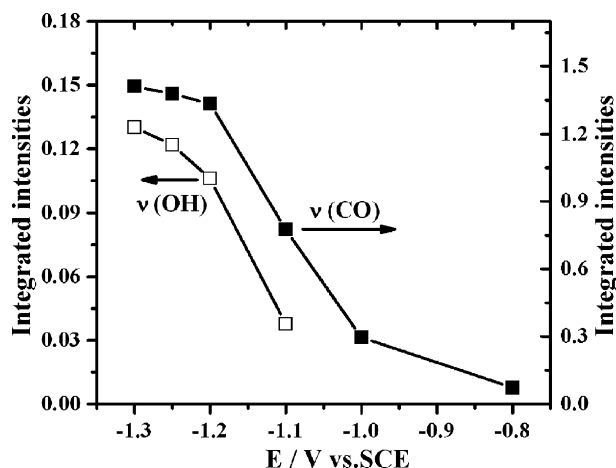


Fig. 6. The potential-dependent integrated intensities of IR bands of CO and coadsorbed H<sub>2</sub>O, re-plotted based on Fig. 5.

was present only at  $-0.9$  V and higher potentials where CO adsorption was negligible, and upon significant CO adsorption at lower potentials, that band disappeared. Hence, the assignment of CuOH<sub>ads</sub> for this band is suspicious. The second, which is more likely, is the interfacial free H<sub>2</sub>O with its hydrogen-bonding broken as a result of CO adsorption. The detailed structure of these free H<sub>2</sub>O molecules at metal/electrolyte interfaces is still open for discussion [53], but free H<sub>2</sub>O co-existed with CO on Cu electrode may be inferred by the concurrent potential dependence of the  $\nu_{\text{OH}}$  and  $\nu_{\text{CO}}$  bands, as can be seen in Fig. 6. Since the  $\delta_{\text{HOH}}$  band of the free H<sub>2</sub>O was weak and hardly separated from that of other H<sub>2</sub>O, it was submerged in the broad band ca.  $1640\text{ cm}^{-1}$  [31,54]. Similar  $\nu_{\text{OH}}$  bands were observed on previous ATR-SEIRAS on CO adsorbed on Pt [26,31,54–55], Pd [30,31], Rh [31], Ru [31] and Ni [33] electrodes, although the peak positions and intensities varied with metal and CO coverage. Notably, such free H<sub>2</sub>O bands have not been detected on a Au electrode at potentials with maximum CO adsorption in an acid solution, possibly because of lower CO coverage, as revealed by *in situ* STM measurement [56].

High SEIRA-activity of as-deposited Cu nanofilms on Si enables to probe varieties of adsorbates at the electrochemical interface. As an initial step along this line, the configuration of adsorbed Py at a Cu electrode was examined. Compared to SERS, SEIRAS has a straightforward surface selection rule and does not require the ORC pretreatment in a chloride electrolyte for activation. Several possible configurations have been suggested for (sub) monolayer Py adsorption on different metal surfaces, including flat-lying, N-end-on, edge-tilted, plane-tilted and  $\alpha$ -pyridyl ones [14–15,18,33,44,57–63]. Haq and King determined a N-end-on configuration for Py on Cu(110) in a UHV system based on external IRAS measurement [44], while based on the SERS selection rule, Zuo and Jagodzinski [18] proposed a predominant formation of  $\alpha$ -pyridyl species on Cu nanoparticles formed on a Al foil by a metathesis reaction. The end-on configuration was also suggested previously on an ORC-roughened Cu electrode by *in situ* SERS studies [14,15]. In the following, we take the advantage of our SEIRA-active Cu nanofilms to clarify these two extreme configurations.

Fig. 7 shows cyclic voltammograms obtained from an as-deposited Cu nanofilm electrode in 0.1 M KClO<sub>4</sub> solution without (solid trace) and with (dashed trace) 10 mM Py. The oxidation of Cu initiated at potentials around  $-0.3$  V in the forward scan, and the hydrogen evolution initiated at potentials around  $-1.0$  V in the negative scan. Obviously, both are suppressed by the presence of 10 mM Py.

Unlike on Au and Ag electrodes [40,62], Py was found to be adsorbed on the Cu electrode over a very wide potential region; it can survive at very negative potentials of strong H<sub>2</sub> evolution. The strong adsorption of Py on Cu prevented from finding a suitable reference potential in the Py-containing solution and thus the corresponding spectra measured in 0.1 M KClO<sub>4</sub> without Py at the same potentials as for the sample spectra were taken as the reference ones, respectively.

Fig. 8 shows a series of *in situ* ATR-SEIRA spectra for a Cu nanofilm electrode in 0.1 M KClO<sub>4</sub> solution containing 10 mM Py. Six bands characteristic of intact pyridine (rather

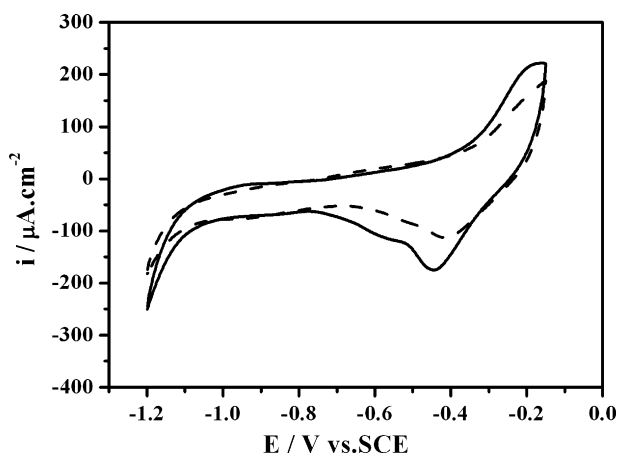


Fig. 7. Cyclic voltammograms of a Cu nanofilm electrode in 0.1 M KClO<sub>4</sub> solution in the absence (solid) and presence (dashed) of 10 mM Py recorded at 50 mV s<sup>-1</sup>.

than  $\alpha$ -pyridyl) adsorbed on a Cu electrode were detected at 1600 ( $\nu_{8a}$ , C–C and C–N stretch, vs), 1482 ( $\nu_{19a}$ , C–C and C–N stretch, s), 1444 ( $\nu_{19b}$ , C–C and C–N stretch, vw), 1068 ( $\nu_{18a}$ , C–H in plane bend, m), 1042 ( $\nu_{12}$ , asymmetric ring breathing, m) and 1013 cm<sup>-1</sup> ( $\nu_1$ , symmetric ring breathing, m) [64,65]. All the bands observed can be classified into A<sub>1</sub> symmetry except the very weak  $\nu_{19b}$  band assignable to B<sub>1</sub> symmetry mode (A<sub>1</sub> and B<sub>1</sub> modes are defined here as in-plane vibrations yielding dipole changes along and perpendicular to the C<sub>2</sub>-axis of Py, respectively). It should be pointed out that the weakest  $\nu_{19b}$  band observed in ATR-SEIRAS is the most intense IR band of all for liquid pyridine. According to the surface selection rule of SEIRAS, the selective enhancement of A<sub>1</sub> modes of adsorbed Py suggests the “end-on” adsorption geometry on Cu electrode via lone pair of N atom without significant edge-tilting of its C<sub>2</sub>-axis. The blue-shift of the totally symmetric ring vibration band ( $\nu_1$ ) further supports the end-on configuration [66,67]. Effort to detect a band for CH out of plane bend (B<sub>2</sub> mode) at ca. 750–850 cm<sup>-1</sup> was hampered by the strong IR absorption of the Si prism itself. Nevertheless, the ATR-SEIRAS of Py on a

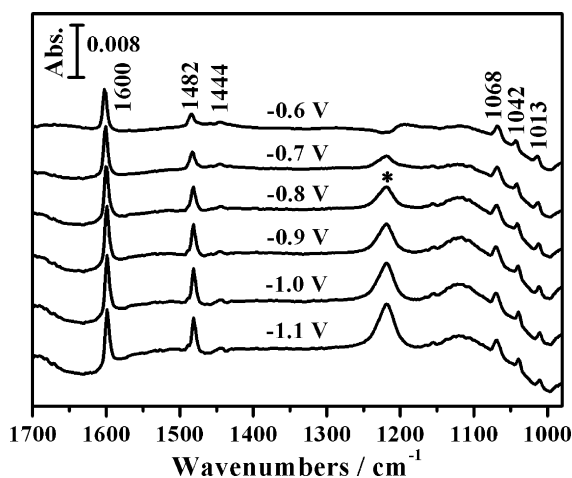


Fig. 8. Potential-dependent SEIRA spectra of Py adsorbed on the Cu electrode in 0.1 M KClO<sub>4</sub> containing 10 mM Py. The reference spectra were the spectra measured in neat 0.1 M KClO<sub>4</sub> at the corresponding potentials as indicated.

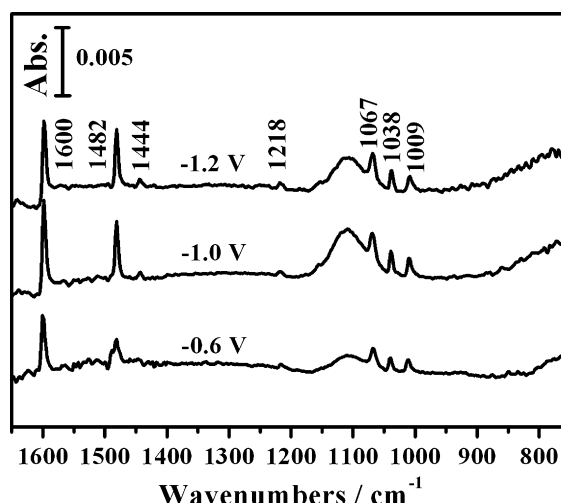


Fig. 9. Potential-dependent SEIRA spectra of pyridine (Py) adsorbed on the Cu electrode chemically deposited on Ge in 0.1 M KClO<sub>4</sub> containing 10 mM Py. Reference spectra were measured in neat 0.1 M KClO<sub>4</sub> at the same potentials as their corresponding sample spectra.

Cu-on-Ge electrode did not detect such a band either as seen in Fig. 9 {note: the weak band at 1218 cm<sup>-1</sup> is also a A<sub>1</sub> mode ( $\nu_{9a}$ )[64,65]}, suggesting that Py ring plane was nearly vertical to the local surface and no Py multilayers were formed [44]. The upright N end-on adsorption configuration agrees with the results observed by IRAS in UHV [44] and *in situ* electrochemical SERS [14,15]. We did not detect any spectral features leading to the possible conclusion of  $\alpha$ -pyridyl species formation on Cu such as the appearance of intense bands with originally B<sub>1</sub> symmetry. In particular, a strong band at ca. 1568 cm<sup>-1</sup>, a marker of the predominant presence of  $\alpha$ -pyridyl observed in previous studies of Py on Pt(1 1 1) [44] and W(1 1 0) [68] in UHV, and Py on a Pt electrode [63], did not show up at all. It is also noted that the band at 1482 cm<sup>-1</sup> gains intensity more rapidly than other A<sub>1</sub> modes as the potential is made more negative, similar to that found in IRAS for Py adsorption on a Cu(1 1 0) in UHV with increasing coverage [44]. The increase in Py coverage with decreasing potential can be understood by the weakened competition from co-adsorbed anions. The reason why vibrations with the same A<sub>1</sub> symmetry were affected to different extents with increasing coverage deserves further consideration in the future.

The broad band at ca.1225 cm<sup>-1</sup> in Fig. 8 is commonly observed for a metal-on-Si electrode especially in an un-acidic solution [21,62–63], but it is absent for a metal-on-Ge electrode (see Fig. 9). This band is much weaker in a strong acid solution like 0.1 M HClO<sub>4</sub> or H<sub>2</sub>SO<sub>4</sub> [31,36,69]. It's tempting to assign it to the O–Si–O stretching of the silicon oxides formed (and/or grown) on the exposed Si sites [70], which is thermodynamically facilitated with increasing local pH upon hydrogen evolution. Another possible candidate species for this band is the silicates formed at certain potentials [36].

#### 4. Conclusions

Based on a seeded-growth tactics, chemical deposition of Cu nanofilm electrodes on Si has been achieved to replace tradi-

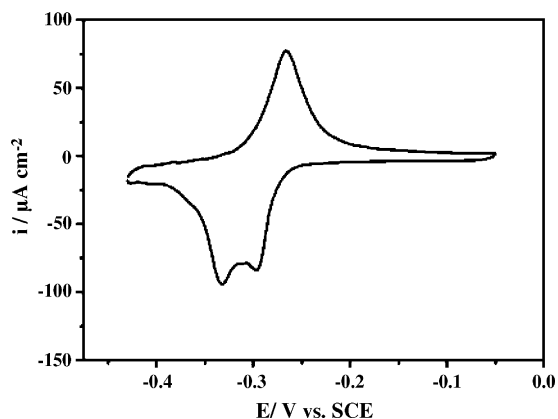


Fig. A.1. Cyclic voltammogram for the UPD of a Pb monolayer on the bulk Cu electrode on Si in deaerated 0.1 M HClO<sub>4</sub> containing 1 mM Pb(ClO<sub>4</sub>)<sub>2</sub>·3H<sub>2</sub>O, the scan rate is 10 mV s<sup>-1</sup>.

tional vacuum deposition for *in situ* ATR-SEIRAS applications. With CO as the probe molecule, the unipolar surface signal is ca. 30-fold stronger than those reported for a bulk Cu electrode in IRAS, facilitating the detection of probable interfacial free H<sub>2</sub>O species. *In situ* ATR-SEIRAS of Py adsorption on a Cu electrode did not support the formation of  $\alpha$ -pyridyl species. An upright N-end-on configuration of Py on Cu was confirmed over the potential range under investigation.

### Acknowledgements

The NSFC (No. 20473025), the SRFDP (No. 20040246008), the NCET (No. 04-0349), the SNPC (No. 0452nm064) and Innovative Fund of Fudan University (CQH1615018), China (WBC), and the MEXT (No. 18350038 and Priority Areas 417), Japan (MO) are gratefully acknowledged for financial supports. We also thank the State Key Laboratory for Physical Chemistry of Solid Surfaces, Xiamen University for providing partial financial support through the Coordinator, Prof. Z. Q. Tian (No. 200303).

### Appendix A

See Fig. A.1.

### References

- [1] D. Rezaekhani, A.A. Zhaam, Proceedings of the 15th International Corrosion Congress: Frontiers in Corrosion Science and Technology, Granada, Spain, 2002, p. 22.
- [2] Boffardi, P. Bennett, *Power* 129 (1985) 57.
- [3] S.P. Murarka, *Mater. Sci. Eng. R.* 19 (1997) 87.
- [4] R. Rosenberg, D.C. Edelstein, C.K. Hu, K.P. Rodbell, *Ann. Rev. Mater. Sci.* 30 (2000) 229.
- [5] A.D. Modestov, G.D. Zhou, Y.P. Wu, T. Notoya, D.P. Schweinsberg, *Corros. Sci.* 36 (1994) 1931.
- [6] K.P. Ishida, P.R. Griffiths, *Anal. Chem.* 66 (1994) 52.
- [7] B. Bozzini, V. Romanello, G.P. De Gaudenzi, C. Mele, *Trans. Inst. Met. Finish.* 84 (2006) 154.
- [8] S. Kaneco, K. Iiba, H. Katsumata, T. Suzuki, K. Ohta, *Electrochim. Acta* 51 (2006) 4880.
- [9] F. Armijo, M. Isaacs, G. Ramirez, E. Trollund, J. Canales, M.J. Aguirre, *J. Electroanal. Chem.* 566 (2004) 315.
- [10] M.Z. Luo, R.P. Baldwin, *J. Electroanal. Chem.* 387 (1995) 87.
- [11] A.J. Bard, L.R. Faulkner, *Electrochemical Methods—Fundamentals and Applications*, John Wiley & Sons, New York, 1980.
- [12] V.D. Jovic, B.M. Jovic, *J. Electroanal. Chem.* 541 (2003) 13.
- [13] R.K. Chang, T.E. Furtak, *Surface Enhanced Raman Scattering*, Plenum Press, New York, 1982.
- [14] A. Bruckbauer, A. Otto, *J. Raman Spectrosc.* 29 (1998) 665.
- [15] J.S. Gao, Z.Q. Tian, *Chem. Phys. Lett.* 262 (1996) 151.
- [16] H.Y.H. Chant, M.J. Weaver, *Langmuir* 15 (1999) 3348.
- [17] Z.Q. Tian, B. Ren, D.Y. Wu, *J. Phys. Chem. B* 106 (2002) 9463.
- [18] C. Zuo, P.W. Jagodzinski, *J. Phys. Chem. B* 109 (2005) 1788.
- [19] B. Bozzini, C. Mele, L. D'urzo, V. Romanello, *J. Appl. Electrochem.* 36 (2006) 973.
- [20] J. Lipkowski, L. Stolberg, J. Lipkowski, in: P.N. Ross (Ed.), *Adsorption of Molecules at Metal Electrodes*, VCH, New York, 1992, p. 171.
- [21] M. Osawa, J.M. Chalmers, in: P.R. Griffiths (Ed.), *Handbook of Vibrational Spectroscopy*, vol. 1, John Wiley & Sons, Chichester, UK, 2002, p. 785.
- [22] T. Wandlowski, K. Ataka, S. Pronkin, D. Diesing, *Electrochim. Acta* 49 (2004) 1233.
- [23] A.E. Jerke, P.R. Griffiths, W. Theiss, *Anal. Chem.* 71 (1999) 1967.
- [24] H. Miyake, S. Ye, M. Osawa, *Electrochem. Commun.* 4 (2002) 973.
- [25] A. Miki, S. Ye, M. Osawa, *Chem. Commun.* (2002) 1500.
- [26] Y.X. Chen, A. Miki, S. Ye, H. Sakai, M. Osawa, *J. Am. Chem. Soc.* 125 (2003) 3680.
- [27] A. Rodes, J.M. Orts, J.M. Perez, J.M. Feliu, A. Aldaz, *Electrochem. Commun.* 5 (2003) 56.
- [28] A. Miki, S. Ye, T. Senzaki, M. Osawa, *J. Electroanal. Chem.* 563 (2004) 23.
- [29] H. Miyake, M. Osawa, *Chem. Lett.* 33 (2004) 278.
- [30] S. Pronkin, T. Wandlowski, *Surf. Sci.* 573 (2004) 109.
- [31] Y.G. Yan, Q.X. Li, S.J. Huo, M. Ma, W.B. Cai, M. Osawa, *J. Phys. Chem. B* 109 (2005) 7900.
- [32] J.M. Delgado, J.M. Orts, A. Rodes, *Langmuir* 21 (2005) 8809.
- [33] S.J. Huo, X.K. Xue, Y.G. Yan, Q.X. Li, M. Ma, W.B. Cai, Q.J. Xu, M. Osawa, *J. Phys. Chem. B* 110 (2006) 4162.
- [34] Y.X. Chen, M. Heinen, Z. Jusys, R.J. Behm, *Angew. Chem., Int. Ed.* 45 (2006) 981.
- [35] Y.X. Chen, M. Heinen, Z. Jusys, R.J. Behm, *Langmuir* 22 (2006) 10399.
- [36] H. Miyake, E. Hosono, M. Osawa, T. Okada, *Chem. Phys. Lett.* 428 (2006) 451.
- [37] Y.X. Diao, M.J. Han, L.J. Wan, K. Itaya, T. Uchida, H. Miyake, A. Yamakata, M. Osawa, *Langmuir* 22 (2006) 3640.
- [38] A. Yamakata, T. Uchida, J. Kubota, M. Osawa, *J. Phys. Chem. B* 110 (2006) 6423.
- [39] K. Kunimatsu, H. Uchida, M. Osawa, M. Watanabe, *J. Electroanal. Chem.* 587 (2006) 299.
- [40] S.J. Huo, X.K. Xue, Q.X. Li, S.F. Xu, W.B. Cai, *J. Phys. Chem. B* 110 (2006) 25721.
- [41] L.A. Porter, H.C. Choi, A.E. Ribbe, J.M. Buriak, *Nano Lett.* 2 (2002) 1067.
- [42] D. Xu, E.T. Kang, K.G. Neoh, Y. Zhang, A.A.O. Tay, S.S. Ang, M.C.Y. Lo, K. Vaidyanathan, *J. Phys. Chem. B* 106 (2002) 12508.
- [43] N.M. Hasan, S.G.D. Filho, W. Schwarzacher, *Electrochem. Solid-State Lett.* 8 (2005) C145.
- [44] S. Haq, D.A. King, *J. Phys. Chem.* 100 (1996) 16957.
- [45] W. Kern, D.A. Puotinen, *RCA Rev.* 31 (1970) 187.
- [46] K. Ataka, T. Yotsuyanagi, M. Osawa, *J. Phys. Chem.* 100 (1996) 10664.
- [47] R. Vasilic, N. Vasiljevic, N. Dimitrov, *J. Electroanal. Chem.* 580 (2005) 203.
- [48] A. Lukomska, J. Sobkowski, *J. Electroanal. Chem.* 567 (2004) 95.
- [49] J. Salimon, R.M. Hernandez-Romero, M. Kalaji, *J. Electroanal. Chem.* 538 (2002) 99.
- [50] O. Koga, T. Matsuo, N. Hoshi, Y. Hori, *Electrochim. Acta* 44 (1998) 903.
- [51] Y. Hori, H. Wakebe, T. Tsukamoto, O. Koga, *Surf. Sci.* 335 (1995) 258.
- [52] Y. Hori, O. Koga, H. Yamazaki, T. Matsuo, *Electrochim. Acta* 40 (1995) 2617.
- [53] A. Cuesta, *J. Electroanal. Chem.* 587 (2006) 329.
- [54] M. Futamata, L.Q. Luo, C. Nishihara, *Surf. Sci.* 590 (2005) 196.
- [55] T. Yajima, H. Uchida, M. Watanabe, *J. Phys. Chem. B* 108 (2004) 2654.

- [56] C.H. Shue, L.Y.O. Yang, S.L. Yau, K. Itaya, *Langmuir* 21 (2005) 1942.
- [57] P. Zelenay, L.M. Rice-Jackson, A. Wieckowski, *Langmuir* 6 (1990) 974.
- [58] J. Lipkowski, L. Stolberg, S. Morin, D.E. Irish, P. Zelenay, M. Gamboa, A. Wieckowski, *J. Electroanal. Chem.* 355 (1993) 147.
- [59] J. Lipkowski, L. Stolberg, D.F. Yang, B. Pettinger, S. Mirwald, F. Henglein, D.M. Kolb, *Electrochim. Acta* 39 (1994) 1045.
- [60] A.G. Brolo, D.E. Irish, J. Lipkowski, *J. Phys. Chem. B* 101 (1997) 3906.
- [61] N.H. Li, V. Zamlynyy, J. Lipkowski, F. Henglein, B. Pettinger, *J. Electroanal. Chem.* 524 (2002) 43.
- [62] W.B. Cai, L.J. Wan, H. Noda, Y. Hibino, K. Ataka, M. Osawa, *Langmuir* 14 (1998) 6992.
- [63] Y.G. Yan, Q.J. Xu, W.B. Cai, *Acta Chim. Sinica.* 64 (2006) 458.
- [64] L. Corrsin, B.J. Fax, R.C. Lord, *J. Chem. Phys.* 21 (1953) 1170.
- [65] C.H. Kline Jr., J. Turkevich, *J. Chem. Phys.* 12 (1944) 300.
- [66] A. Otto, I. Mrozek, H. Grabhorn, W. Akemann, *J. Phys.: Condes. Matter.* 4 (1992) 1143.
- [67] H. Metiu, *Prog. Surf. Sci.* 17 (1984) 153.
- [68] M.P. Andersson, P. Uvdal, *J. Phys. Chem. B* 105 (2001) 9458.
- [69] S.J. Huo, Q.X. Li, Y.G. Yan, Y. Chen, W.B. Cai, Q.J. Xu, M. Osawa, *J. Phys. Chem. B* 109 (2005) 15985.
- [70] V.P. Tolstoy, I.V. Chernyshova, V.A. Skrushevsky, *Handbook of Infrared Spectroscopy of Ultrathin Films*, John Wiley & Sons, Inc., New York, 2003.